AIAA 2013-1384

Fluid Structure Interaction Parachute Benchmark Models in LS-DYNA®

Ben Tutt[1]
Airborne Systems North America, Santa Ana, CA, 92704

This paper describes the development and results of numerical models describing system level parachute performance. The numerical models were developed to replicate a series of parachute drop tests conducted in the early 1950s. Wright Air Development Division Report AFTR 5867 documents 700 parachute drop tests, using twenty seven different parachutes, at the Goodyear Aircraft Corporation airship dock in Akron, Ohio between 1952 and 1954. The data from these tests were compiled into charts and referenced in the Parachute Recovery Systems Design Manual (T.W. Knacke). The numerical models were developed using Fluid Structure Interaction (FSI) techniques in the commercially available transient dynamic finite element code LS-DYNA. This paper describes the development of an 11.9 ft Nominal Diameter (D_0) 10% extended skirt parachute model. Parachute drag, maximum oscillation angle, and frequency of oscillation are calculated for the parachute for ranges of rate of descent and suspension line length ratio, and compared with test data from AFTR 5867. This paper proposes a benchmarking parachute test series for current and future FSI numerical models.

Nomenclature

C_D	=	drag coefficient based on the nominal diameter
D_0	=	nominal diameter as determined from the total canopy area
F	=	drag force
FSI	=	Fluid Structure Interaction
L_s	=	suspension line length
q	=	dynamic pressure
S_0	=	total canopy area

I. Introduction

DESIGN analysis of parachute recovery systems has relied on a combination of core design principles, historical empirical data, and extensive testing since the days of World War II. The complex aerodynamics and structural dynamics of a highly deformable and flexible fabric system are numerous and have limited the advancement of a truly quantitative design analysis approach.

There are many features of a parachute system that are unique within typical engineering analysis and which require specialized or uniquely focused numerical analysis. A key operational performance parameter of a parachute is the extent to which it can change its volume within the shortest period of time; a modern large parachute will change its volume by a factor of 7000 within seconds. Another is the intricate relationship between fabric permeability and applied tension, including the direction of that tension, and the associated connection to parachute inflation forces. It has long been recognized that in order to improve the accuracy and therefore relevancy of parachute system engineering analysis the aerodynamics and structural dynamics of a parachute system need to be the outputs of an analysis rather than the inputs[1,2]. But even though advanced modeling has been under development for the past four decades, progress has been slow and the narrow focus of the efforts often means that the results rarely find a way into an integrated engineering design practice. The reasons for this lack of progress are investigated and discussed in great detail in Ref 3. This paper proposes the use of a series of benchmarking models, and associated test data, which can be used to evaluate numerical models at a system performance level- a level that can be clearly and visibly assessed by the parachute industry. The Parachute Recovery Systems Design Manual, by T.W. Knacke[4] was used to research parachute test data sources that could be used as reference material for this

[1] Systems Analyst, Airborne Systems, 3000 Segerstrom Ave, Santa Ana, CA 92704. AIAA Senior Member.

computational task. The criteria for the selection of a broad test series was to enable the generation of FSI models for comparison with basic top level parachute performance parameters demonstrated in test data. Such top level parameters are the relationships between payload mass or parachute suspension line length on parachute drag efficiency, or on the stability of the parachute system. By focusing on the system level performance parameters it will enable the parachute designer to gain a better understanding of the current state of the art of parachute analysis codes. The ability to identify design trends and patterns in a numerical model can be very useful to the parachute designer, who perhaps is not as concerned about identifying the drag coefficient to three decimal places or the load in a suspension line to within 5%. For many parachute applications and from a design efficiency perspective, it is important that numerical models provide an understanding of parachute performance and highlight critical design considerations, without burdening the modeling with having to directly replicate quantitative performance. For the majority of applications it is the last 5% of accuracy that consumes, in both time and complexity, 90% of the resources. Clearly, for some parachute systems or specific applications it is highly critical that the predictions are incredibly accurate, however not every analysis should be held to that same level of precision.

II. Parachute Test Data

The performance data measured during a parachute test series is invariably connected to the product or requirements of the source funding the test series. It is increasing rare in modern times to find a funding source that is simply interested in generating a broad source of parachute design data, more common is a test series that is aimed at developing or maturing a particular design. Once a design is shown to sufficiently meet the requirements the testing is completed and documented in a manner commensurate with the program. Several recent U.S Government funded programs have generated significant and broad performance data for sub-scale parachutes in a controlled environment[5] and extensive development and qualification testing for large ringsail parachutes[6].

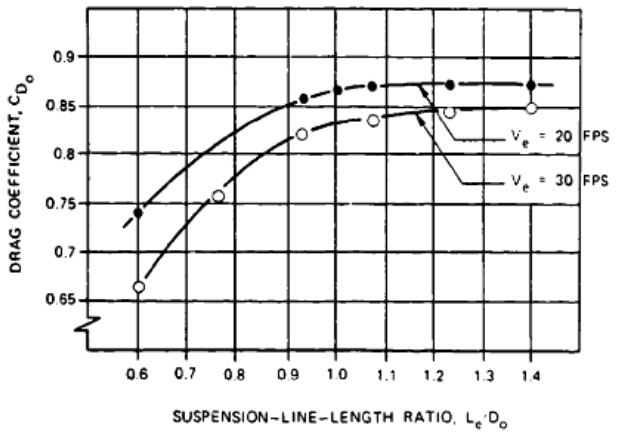

FIGURE 5-26. Effect of Suspension-Line Ratio on an 1.8-Foot-Diameter Extended-Skirt Parachute.

Figure 1. Influence of Suspension Line Length on Drag Coefficient

The Parachute Recovery Systems Design Manual was used to research parachute test data sources that could be used as reference material for this computational task. Many of the Design Manual references are either not available or consist of insufficient data to replicate test conditions or parachute configurations. Following an assessment of available references the drop test data documented in AFTR 5867, *Drop Tests of 16,000 Square-Inch Model Parachutes*, F.J. Stimler and R.S. Ross (Ref. 7) proved to be the most extensive and comprehensive. Air Force Technical Report 5867 is a Wright Air Development Division report that documents 700 parachute drop tests conducted at the Goodyear Aircraft Corporation airship dock in Akron, Ohio in the early 1950s. The purpose of the drop test program was to determine the influence of the canopy type and the rate of descent on the drag and stability characteristics of specific types of parachutes.

A selection of data from that source is reproduced in Fig 5-26 of the Parachute Recovery Systems Design Manual. Figure 5-26 from the Design Manual is replicated in Figure 1. However, even this data source was initially misleading; although labeled in the Design Manual as pertaining to a 1.8 ft diameter extended skirt parachute the reference material confirms that is a typographical error and the parachute tested was an 11.8 ft diameter extended skirt parachute. This figure demonstrates the relationship between drag coefficient and suspension line length and also system velocity. It highlights the drag increase observed as the suspension lines of the extended skirt parachute are increased, but also that the efficiency is asymptotic and beyond a certain line length the benefits are negligible. It also shows how the payload mass and therefore descent velocity impacts the drag efficiency of the parachute. These relationships have become core parachute design principles and are now applied across a range of parachutes, loading conditions, and construction techniques.

Figure 2 is an illustration from AFTR 5867 depicting the drop test set-up. The performance of 27 different parachutes were measured to investigate the influence of parachute shape, payload mass, and suspension line length ratio on parachute stability and drag. Each parachute had a total surface area of approximately 16,000 in^2, equating to a nominal diameter of 142.7 in. The following parachute types were assessed: solid flat, solid extended skirt, solid spherical, solid conical, airfoil, Exeter Type 12, guide surface, ringslot, and FIST ribbon. For the purposes of this numerical study the scope has been constrained to the solid extended skirt canopy type.

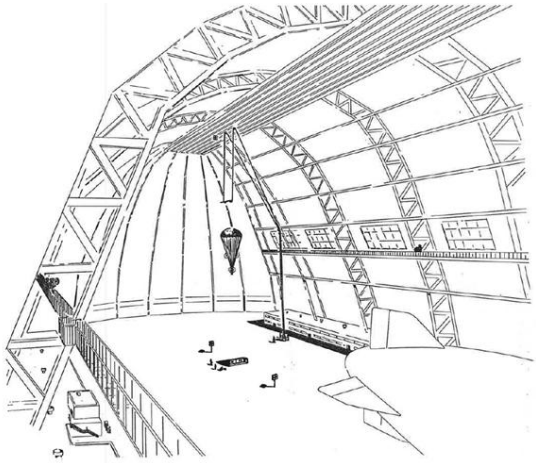

Figure 2. Goodyear Aircraft Parachute Test Set-up

III. Model Development

The commercially available transient dynamic finite element code LS-DYNA was utilized to develop models for this study.

The numerical approach discussed in this paper utilizes a first order Eulerian temporal solution with a second order accurate advection method. An Eulerian formulation on a Cartesian mesh is used for the fluid, Lagrangian 4-noded membrane elements based on the Belytschko-Lin-Tsay formulation for the parachute structural mesh, and a quasi-penalty based porosity coupling method was employed to enable the two to interact. The use of an Eulerian-Lagrangian coupling algorithm permits the interaction of the fluid and structure to occur within the same computational solver and completely avoids the numerical problems associated with distortions of the fluid mesh. Following the classification discussed in Ref. 3 this coupling would be described as "partitioned" and "loose". Partitioned meaning that the fluid and structural fields are solved separately and forces, velocities, and displacements are passed through an interface- in this case the *CONSTRAINED_LAGRANGE_IN_SOLID card, and loose meaning that the fluid and structure equations are solved once during each time-step. However, it should be noted that both the fluid and structural fields are solved within the same LS-DYNA code environment, i.e. completely separate codes are not used for this analysis.

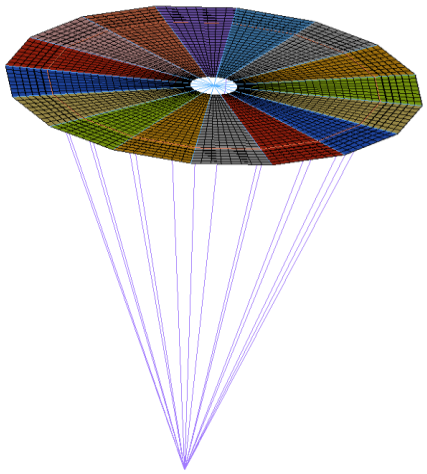

Figure 3. Parachute Structural Model

The computational model developed for this study consists of a separate parachute structural model, and a fluid model. The parachute model is based on the T-10 extended skirt model previously developed and documented in Ref. 8. Figure 3 illustrates the structural model of the 11.9 ft D_0 10% extended skirt parachute; the extended skirt is shown folded under the rest of the canopy. Table III-1 summarizes the parachute construction details.

Table III-1. Parachute Model Parameters

Parachute Type	Total Surface Area (in^2)	Vent Area (in^2)	Number of Gores	Number of Suspension Lines	Parachute Gore Cloth	Parachute Line Material
10% Extended Skirt	16,000	160	16	16	Rip Stop Nylon*	100 lbf Nylon**

* Bureau of Aeronautics Specification 27N4 (Aer.)

** Specification AN-C-63a Type I

The parachute model is constructed from 4,096 Lagrangian 4-noded membrane elements based on the Belytschko-Lin-Tsay formulation, and 896 2-noded seatbelt cable elements that are used to model the suspension lines, skirt band, vent band, and vent lines.

The Eulerian fluid is modeled in a spatially fixed Cartesian mesh. This is often referred to as a wind tunnel class model; the confluence of the lines is restricted and air is forced into and around the parachute at a known velocity and density. The application of Eulerian formulations can lead to a propensity for energy dissipation and dispersion inaccuracies connected with the fluxing of mass across element boundaries. In addition, the Eulerian mesh is required to span the entire range of activity associated with the Lagrangian structure. In many applications, this can result in a large size mesh and hence a high computing cost. Many of these potential difficulties have been managed through algorithm development and vast improvements in computing power. Ballistic parachutes are relatively unique aerodynamic devices that are designed to generate drag and as such their bluff body form is ideally suited to Euler based solutions.

Figure 4 depicts the fluid mesh developed for this study. The mesh comprises 691,740 solid hexahedral elements that have all 6 degrees of freedom at every node. Nodes around the circumference of the fluid mesh are prescribed a slip condition. The parachute image shown in Figure 4 is at the end of the simulation and shows the inflated and deformed shape caused by the air flow. The time zero parachute geometry, the input to the model, is depicted in Figure 3.

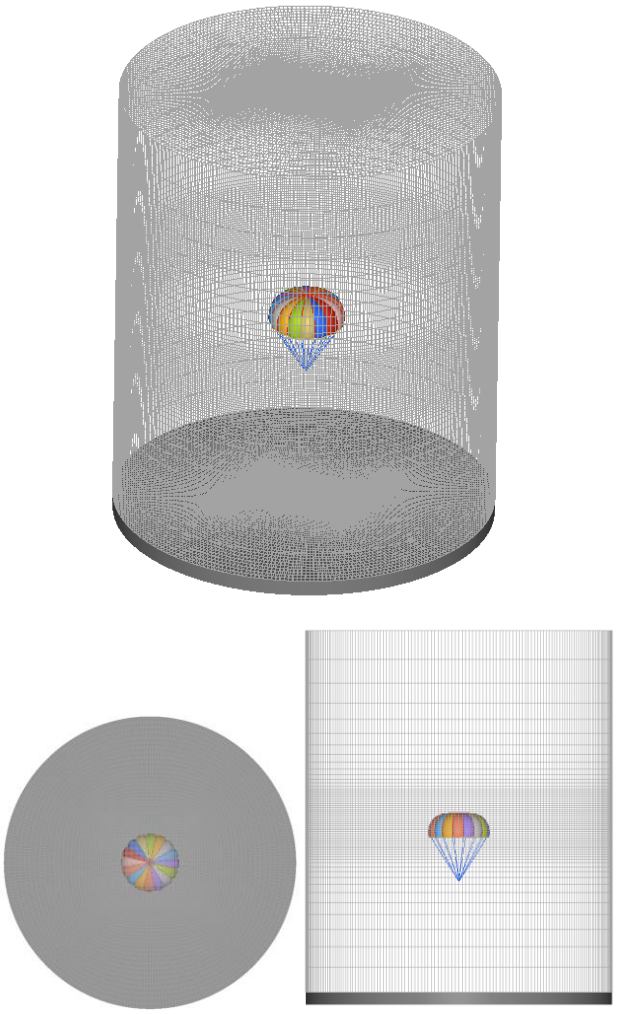

Figure 4. Computational Fluid Mesh with Parachute Structural Model inside.

Constant and uniform fluid flow conditions were prescribed to the bottom row of nodes in the computational mesh, shown in the right image of Figure 4. These flow conditions were dependent on the model being evaluated, ranging from 12 ft/s to 40 ft/s.

Parachute drag force (F) was recorded at the confluence of the suspension lines for variations in prescribed flow velocity (12 ft/s, 26 ft/s, and 40 ft/s) at MSL density (together defining q), which combined with the parachute reference area will be used to directly calculate drag coefficient using the equation below:

$$C_D = \frac{F}{S_0 \cdot q} \qquad \text{Eq. (1)}$$

The lengths of the suspension lines were modified and the models resolved to provide a measure of the influence of suspension line length on parachute drag and stability. Line length ratios of 0.60 and 0.92 have been assessed in the models. Line length ratio is defined as L_s/D_o.

The nodal location of the parachute apex was tracked throughout each simulation and used to measure the oscillation angle of the parachute as a function of time. This data was used to record average oscillation angle and frequency of oscillation.

IV. Drop Test Results

Volume VIII of Ref. 7 summarizes the performance of the extended skirt parachute as:

> *"These parachutes exhibit gliding tendencies at the lower vertical velocity range, and descended approximately vertically with large oscillation at the upper vertical velocity range……. Cd ranged from 0.86 to 0.65 decreasing in value for a decrease in suspension line ratio."*

Table IV-1 summarizes the test data from eight parachute drops of the 10% extended skirt solid-flat parachute. The data in Table IV-1 is taken from Table 5d and Table 5f from Ref.7. The data includes drag and stability performance of the extended skirt parachute with two different suspension line lengths. Drop #s 145-154 incorporated suspension lines that were 10 ft 11 in long, and Drop #s 193-202 incorporate lengths of 7 ft 2 in long.

Table IV-1. Summary of Drop Test Data

Drop #	L_s/D_o	Vertical Terminal Velocity (ft/s)	Cd	Frequency of Oscillation (cycles per sec)	Maximum Angle of Oscillation (deg)	Average Angle of Oscillation (deg)
145	0.92	10.7	1.048	0.286	25	25
149	0.92	16.5	0.870	0.286	31	22
153	0.92	27.0	0.817	0.400	33	27
154	0.92	41.5	0.908	0.445	31	27
193	0.60	11.9	0.845	0.200	23	20
197	0.60	17.7	0.766	-	18	10
199	0.60	29.2	0.686	0.333	28	25
202	0.60	45.2	0.700	-	17	-

The test data indicates that:

- Drag coefficient is higher for greater line lengths
- Frequency of oscillation is higher for greater line lengths
- The drag coefficient increases as the velocity goes down for both line lengths
- The frequency of oscillation goes down as the velocity goes down for both line lengths
- The maximum and average angle of oscillation follows no firm and discernible pattern

Figure 5 shows summary parachute performance curves from Ref. 7. These curves were purposefully reproduced alongside the actual data (Table IV-1) to highlight the conclusions drawn from the actual scattered data and the judgment inherent in simplifying such data into a curve as shown Figure 5.

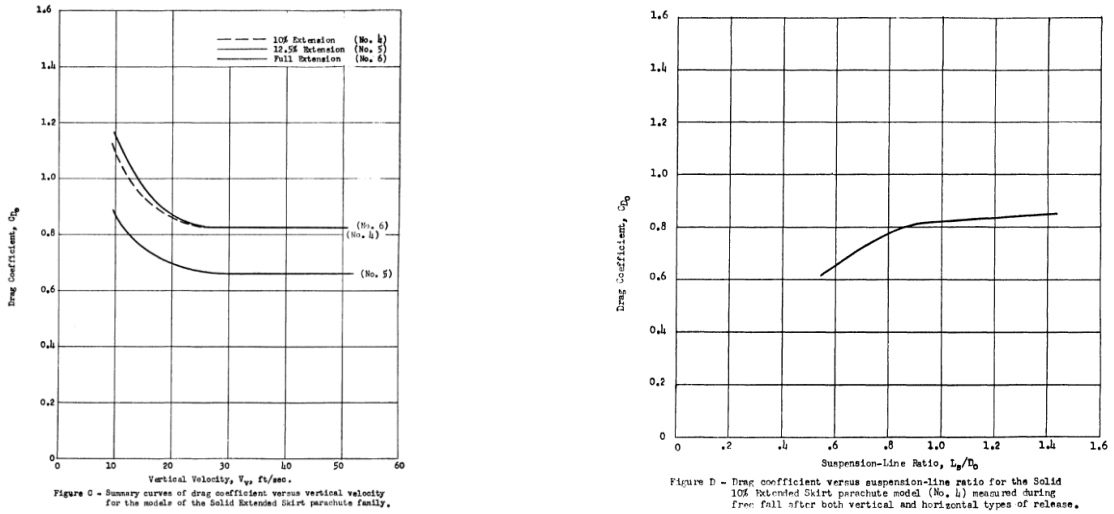

Figure C - Summary curves of drag coefficient versus vertical velocity for the models of the Solid Extended Skirt parachute family.

Figure D - Drag coefficient versus suspension-line ratio for the Solid 10% Extended Skirt parachute model (No. 4) measured during free fall after both vertical and horizontal types of release.

Figure 5. Summary Performance Curves, Reproduced from Ref. 7.

V. Model Results

Separate models were executed for six out of the eight conditions described in Table IV-1. The models were run on a Dell PowerEdge machine using 32 cores, and LS-DYNA executable 971 R6.1 Revision 77948 with Platform MPI v8.02.

Each model covered between 8 and 20 seconds of real world performance time, based on reaching a stable performance. Each second of real world time taking 112 minutes of computational time; 20 seconds of parachute performance took 2240 minutes or 37 hours.

Error! Reference source not found. and Table V-2 document the model results in red and the test results in black, for line length ratios of 0.92 and 0.60, respectively. Figure 6 through
Figure 8 chart test data and model results for drag coefficient, oscillation frequency, and oscillation angle. The models do not cover the period of operation where the maximum angle of oscillation occurs, so no comparison is made with test data.

Table V-1. Comparison of Test and Model Results, Ls/Do = 0.92

Drop #	Vertical Terminal Velocity (ft/s)	C_D	Frequency of Oscillation (cycles per sec)	Maximum Angle of Oscillation (deg)	Average Angle of Oscillation (deg)
145	10.7 10.7	1.048 1.06	0.286 0.15	25	25 20
149	16.5	0.870	0.286	31	22
153	27.0 25.4	0.817 0.81	0.400 0.28	33	27 24
154	41.5 39.8	0.908 0.78	0.445 0.46	31	27 25

Table V-2. Comparison of Test and Model Results, Ls/Do = 0.60

Drop #	Vertical Terminal Velocity (ft/s)	C_D	Frequency of Oscillation (cycles per sec)	Maximum Angle of Oscillation (deg)	Average Angle of Oscillation (deg)
193 2-1	11.9 10.6	0.845 0.81	0.200 0.16	23 -	20 26
197	17.7	0.766	-	18	10
199 2-2	29.2 25.5	0.686 0.66	0.333 0.42	28	25 22
202	45.2	0.700	-	17	-

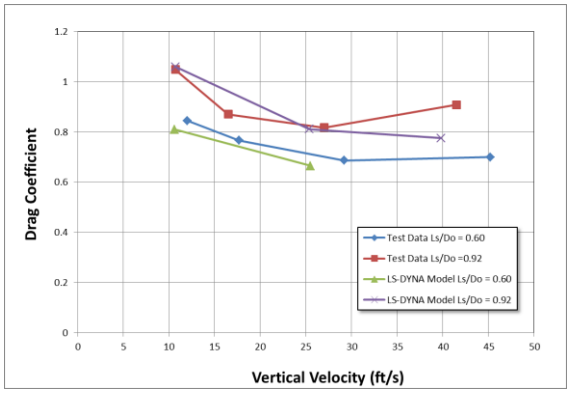

Figure 6. Comparison of Test and Model Results, Drag Coefficient vs. Vertical Velocity

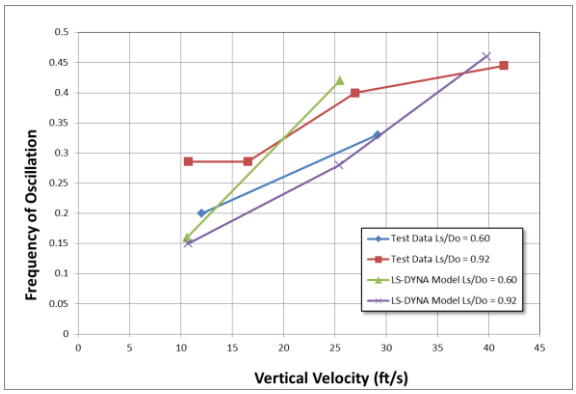

Figure 7. Comparison of Test and Model Results, Frequency of Oscillation vs. Vertical Velocity

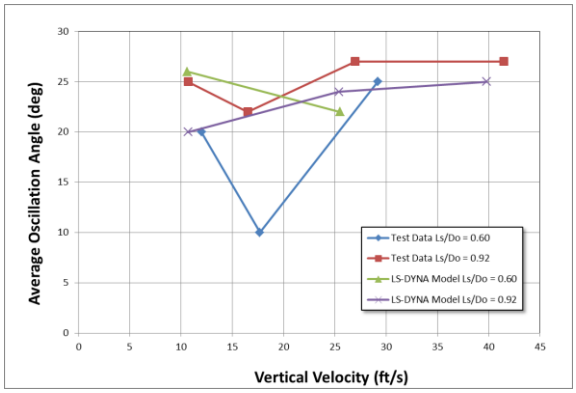

Figure 8. Comparison of Test and Model Results, Average Oscillation Angle vs. Vertical Velocity

Figure 6 compares the drop in drag coefficient as the vertical velocity increases. This can be thought of as the reduction in the effectiveness of the parachute as the payload becomes heavier. The curves also indicate the reduction in drag efficiency for the shorter suspension lines. The LS-DYNA model accurately identifies the drag coefficient trend for both a change in suspension line length and vertical velocity. It is noticeable that the test data with L_s/D_o = 0.92 shows a small increase in drag coefficient at the highest descent velocity. This is not resolved in the LS-DYNA model and similarly is not shown in the summary curves that are presented in Ref. 7.

The stability results, oscillation frequency and average angle, provide a less distinct pattern in both the test data and model. The primary trend of the frequency of oscillation, as shown in Figure 7, is that the frequency increases with vertical velocity (payload mass). This trend is identified in both the test data and model. The correlation with suspension line length is less clear, the test data indicates that longer lines marginally increases frequency, whereas the model indicates the opposite is true above a certain vertical velocity.

Figure 8 compares average oscillation angle as a function of vertical velocity and suspension line length. The test data and model indicate that the oscillation angle varies only marginally with both system parameters. However, it is noticeable that a clear dip in oscillation angle, reflecting a position of greater stability is observed at approximately 17 ft/s vertical velocity. This is an important conclusion and indicates that an optimum payload mass is obtainable for this parachute with respect to system stability. Future work could involve running the models at this interim vertical velocity to see if it also predicts this position of greater stability.

VI. Conclusion

This study has highlighted the capability of LS-DYNA models to predict system-level parachute drag and stability performance. The models are clearly able to assess the influence that parachute line length and system descent velocity have on parachute drag and oscillation angle. Good correlation has been demonstrated with parachute drag test data, with less clear but similar correlation with system stability.

The magnitude and pattern of the drag coefficient was accurately predicted by the model. A clear reduction in drag efficiency was discernible as the line length was reduced and vertical velocity was increased.

The magnitude of the model oscillation frequency and oscillation angle was similar to the test data. The model followed the same general trend as the oscillation frequency observed in the test data with both sources depicting an increase in oscillation frequency as the vertical velocity increased. No strong discernible pattern was observed in either source regarding the oscillation angle, although both appeared to indicate there was a particular mid-range vertical velocity that would exhibit increased stability.

It was noticeable during this comparison effort that the summary curves presented by the authors of the original drop test report where ideal depictions of the test data. When the actual test data are added to those curves the scatter in the test data becomes more pronounced. It appears that at the time of the original data analysis the authors made inherent decisions to dismiss outliers and anomalies and draw conclusions based on common sense and engineering judgment using the test data in entirety. Those summary curves, as a result of being in the Parachute Design Manual, are now used frequently to reinforce many different parachute design decisions such as the length of suspension lines.

Acknowledgments

The author would like to acknowledge the support and funding from U.S. Army Natick Soldier Research, Development & Engineering Center (NSRDEC). NSRDEC provided funding for some of the work presented in this paper, and have supported the development of this modeling technique over the past eight years.

References

[1]Maydew, R. C.; Peterson, C. W., "Design and Testing of High-Performance Parachutes (La Conception et les Essais des Parachutes a Hautes Performances)". *Advisory Group for Aerospace Research and Development*; 1991.

[2]Strickland, J. H., Higuchi, H., "Parachute aerodynamics - An assessment of prediction capability". Journal of Aircraft. Vol. 33, No. 2, 1996 pp., 241-252.

[3]Potvin, J., Bergeron, K., Brown, G., Charles, R., Desabrais, K., Johari, H., Kumar, V., McQuilling, M., Morris, A., Noetscher, G., Tutt, B., "The Road Ahead: A White Paper on the Development, Testing and Use of Advanced Numerical Modeling for Aerodynamic Decelerator Systems Design and Analysis' *AIAA Aerodynamic Decelerator Systems Technology Conference*, Dublin, Ireland, 2011.

[4]Knacke, T., W., *Parachute Recovery Systems Design Manual*; Para Publishing, Santa Barbara, California, 1991.

[5]Desabrais, K. J., et al, "Experimental Parachute Validation Research Program and Status Report on Indoor Drop Tests,". AIAA-2007-2500, 19th AIAA Aerodynamic Decelerator Systems Technology Conference and Seminar, 21-24 May 2007 Williamsburg, Virginia.

[6]Morris, A., et al, "Summary of CPAS Gen II Testing Analysis Results". AIAA-2011-2585, 21st AIAA Aerodynamic Decelerator Systems Technology Conference and Seminar, 23-26 May 2011 Dublin, Ireland.

[7]Stimler, F.J., Ross, R.S., "Drop Tests of 16,000 Square-Inch Model Parachutes". Wright Air Development Division Report AFTR 5867, April 1960.

[8]Tutt, B. A., et al, "The Use of LS-DYNA to Assess the Performance of Airborne Systems North America Candidate ATPS Main Parachutes," AIAA-2005-1608, 18th AIAA Aerodynamic Decelerator Systems Technology Conference and Seminar, 23-26 May 2005 Munich, Germany.